



ELSEVIER

Contents lists available at ScienceDirect

## Mechanics of Materials

journal homepage: [www.elsevier.com/locate/mechmat](http://www.elsevier.com/locate/mechmat)

## Viscoelastic adhesive interfacial model and experimental characterization for interfacial parameters

J. Wang<sup>a,b</sup>, Q.H. Qin<sup>c</sup>, Y.L. Kang<sup>a,\*</sup>, X.Q. Li<sup>a</sup>, Q.Q. Rong<sup>a</sup>

<sup>a</sup> Department of Mechanics, Tianjin University, Tianjin 300072, PR China

<sup>b</sup> Department of Mechanics, Hebei University of Technology, Tianjin 300130, PR China

<sup>c</sup> Department of Engineering, Australian National University, Canberra, ACT 0200, Australia

### ARTICLE INFO

#### Article history:

Received 1 July 2009

Received in revised form 22 February 2010

#### Keywords:

Adhesive interfacial model

Viscoelasticity

Experiment-based identification method

Genetic algorithm

### ABSTRACT

In this paper, a three-parameter interfacial model based on Needleman's cohesive theory is presented to characterize the viscoelastic mechanical properties of adhesive structures. For most adhesive structures, the mechanical behavior of adhesive interface layer can be simulated by the proposed adhesive interfacial model. To evaluate effectively the materials parameters of the adhesive layer an improved experiment-based identification method is proposed including four major steps: (1) video-recorded experimental measurement, (2) numerical simulation based on the time-dependent adhesive interfacial model, (3) genetic algorithm, and (4) independent experiment verification. Using the proposed experiment-based identification method, the viscoelastic interfacial mechanical parameters of metal adhesive structures and rubber adhesive structures under tension or shear loading are determined, respectively. Based on the identified parameters, the numerical computational results are in good agreement with the independent experimental measurement results. It seems that the proposed adhesive interfacial model is effective to characterize the mechanical properties of the adhesive layer and the improved experiment-based identification method is promising in solving parameter characterization problems of complex adhesive structures.

© 2010 Elsevier Ltd. All rights reserved.

### 1. Introduction

Adhesive bonding is of interest in a variety of industrial and technological applications such as the automotive, construction, electronic packaging, and aeronautics sectors. In these adhesive structures, the performance of the adhesive interface layer is of crucial importance in providing effective stress transfer. However, damage may easily occur due to stress concentration or bond imperfection under loading. Thus, the mechanical properties of the adhesive interface layer are critical in the design and application of adhesive structural components in general engineering applications.

Over the past decades a number of theoretical and experimental methods have been developed with the aim of investigating the mechanical behavior of adhesive structures under different loading. The embedded-process-zone model (Tvergaard and Hutchinson, 1993, 1996) was one of the approaches used to investigate interfacial fracture of bi-material systems, where a three-parameter traction-separation law together with the opening and shear stress was involved. Wei and Hutchinson (1998) developed an embedded cohesive-zone model for steady-state peeling of a thin elastic-plastic film bonded to an elastic substrate and then conducted parameter characterization using numerical approaches. Yang et al. (1999) used an embedded-process-zone model to study the coupling between interface fracture and plastic strain of the adherend under T-peel test. For the adhesive, a traction-separation law including plasticity was used. Later, Yang et al. (2001)

\* Corresponding author. Tel./fax: +86 22 27403610.  
E-mail address: [tju\\_ylkang@yahoo.com.cn](mailto:tju_ylkang@yahoo.com.cn) (Y.L. Kang).

considered the same traction-separation law for elastic-plastic mode-II crack growth modeling in which Eng-Notched Flexure specimens subjected to a bending load were used to validate the model. Kafkalidis and Thouless (2002) performed a numerical analysis of single-lap shear joints using a cohesive-zone approach. The cohesive-zone model allowed not only the influence of the geometry to be considered, but also included in the analysis the cohesive properties of the interface and plastic deformation of the adherends. Li et al. (2005a) used a cohesive-zone model previously developed by Li et al. (2005b) on adhesively bonded joints to validate both two- and three-parameter laws. Using this method, the strength and deformations were accurately described, as well as the transition between failure of the composite and failure of the interface. The Compact-Tension test was used to determine the properties of the traction-separation laws. Thouless et al. (2006) used a cohesive-zone approach to model the mixed-mode fracture of adhesive GFRP single-lap joints. Using Euler–Bernoulli beam theory, Alfredsson (2003) presented an exact analytical inverse solution to determine the constitutive properties of thin adhesive layers loaded in shear. Recently, Leffler et al. (2007) implemented adhesive layer theory to determine the complete shear stress versus deformation relation of adhesive layer. Gustafson and Waas (2009) investigated the influence of adhesive parameters on the outcome of cohesive-zone finite element simulation. However, the works mentioned above were used only for analyzing the time-independent mechanical properties of adhesive materials. It is especially worth noting that time-dependent mechanical properties are inevitable due to the viscoelasticity of the adhesive layer (Jagota et al., 2000). For the study on dynamic behavior of the adhesive materials, Du et al. (2000) used the linear fracture mechanics for analyzing the time-dependent fracture behavior of Rubber-modified epoxies in experimental tests. Landis et al. (2000) investigated the material separation in the fracture process zone, which is the sum of an elastic and viscoplastic contribution, and cohesive tractions are time-dependent only if plastic opening exists. Liechti and Wu (2001) extracted the time-dependent parameters for the traction-separation law under mixed-mode loading, where the quasi-static debonding between rubber and metal was modeled by non-linear springs and dashpots. Xu et al. (2003a) provided the standard linear solid model to simulate the viscoelastic material behavior, and calibrated the relative parameters by comparing a series of numerical simulations with experimental curves to describe the crack growth in a thermoplastic adhesive (Xu et al., 2003b).

To characterize mechanical properties of structures many experimental procedures were developed during the past decades (see, for example, the classical handbook by Kobayashi, 1987). Among these approaches, the hybrid method (Laermann, 1981) is very effective in characterizing mechanical properties as it relies on the combination of experimental, analytical and numerical methods. Hybrid methods introduced by Laermann are known as “direct method” because they are based on the combined use of experimental, numerical, and theoretical analysis. Experiments may be real experimental measurement or

numerical simulations of experiments (Kobayashi, 1983; Asundi, 1999). By introducing optimization methods into the above mentioned hybrid framework, an effective hybrid/inverse methods were developed. Using the hybrid/inverse method, a great of work were done for the identification of material parameters (Chalal et al., 2004; Molimard et al., 2005; Hartmann et al., 2006; Cooreman et al., 2007; Jiang et al., 2008; Balakrishnan and Socrate, 2008; Davendralingam and Doyle, 2008; Cosola et al., 2008). Considering the importance of experimental measurement, recently, Kang et al. (2004) and Wang et al. (2008) proposed the experiment-based hybrid/inverse method to analyze the material mechanical properties. In this method, the three components say the experimental measurement, numerical simulation and optimization method, were combined integrally based on the experimental measurements.

The focus of this paper is to describe the viscoelastic adhesive interfacial mechanical properties by experimental characterization method. Firstly, a developed three-parameter interfacial model based on Needleman's cohesive model is presented to describe the interfacial mechanical properties of adhesive structures under tension or shear loading. Subsequently, to quantitatively characterize the interfacial parameters of this model, an improved experiment-based identification method is developed. In the process of improved experiment-based identification method, experimental analysis is very important. Experimental data of real structure have been used as the initial data for finite element calculation and the parameter identification procedure. First, a video-recorded experiment system under tension or shear loading is designed and used to obtain the deformation and damage information of the adhesive layer. Meanwhile, on the basis of the proposed viscoelastic adhesive interfacial model, numerical simulations are performed by means of the finite element software ABAQUS and its user-defined element subroutine. Combining the experimental, numerical, and identification technique with an improved genetic algorithm, an experiment-based identification method is constructed for identifying viscoelastic material properties. Numerical results are presented to show the effectiveness and applicability of the proposed method. Finally, independent experimental verification is performed and the results from experimental measurement are compared with those from numerical simulation.

## 2. The viscoelastic adhesive interfacial layer model

To evaluate the viscoelastic interfacial properties of adhesive structural components, an improved viscoelastic adhesive interfacial layer model under tension or shear loading is proposed in this section. In the analysis, the adhesive layer is represented by an improved cohesive zone (Kelvin element). To introduce the viscoelastic factor into this model, a modified exponential cohesive model (Needleman, 1990) which is arranged in parallel with a dashpot is used to characterize the behavior of the adhesive layer.

In the model (Fig. 1), material separation in the normal or tangential direction is considered, respectively. The corresponding constitutive law can be expressed as

$$\sigma = E\varepsilon + \eta\dot{\varepsilon} \tag{1}$$

$$\tau = G\gamma + \mu\dot{\gamma} \tag{2}$$

Taking the mode under shear loading for example, the viscoelastic adhesive interfacial model can be deduced based on the following three assumptions: (a) the stiffness of the Needleman's cohesive-zone model  $d\tilde{T}_t/d\Delta_t$  is used to replace the spring stiffness  $G$  in the Kelvin model. (b) The displacement jump  $\Delta_t$  across the cohesive-zone and the cohesive-surface traction  $T_t$  are used to replace the strain  $\gamma$  and stress  $\tau$  in the Kelvin model. (c) A constant  $\eta_t$  with a unit of force per velocity per area (dashpot coefficient per area) is used to replace  $\eta$  in the Kelvin model with a unit of force per strain rate per area (viscosity). Thus, the corresponding constitutive relation between stress and opening rate is

$$T_t = \tilde{T}_t + \eta_t d\Delta_t/dt \tag{3}$$

In Eq. (3),  $d\Delta_t/dt$  is the opening rate,  $\tilde{T}_t$  is the modified exponential traction-separation law proposed by Needleman (1990). The constitutive equations are as follows:

$$\tilde{T}_t = -\tilde{\tau}_{\max} z e^{\Delta_t/\delta_{tc}} \exp(-z\Delta_t/\delta_{tc}) \quad (\Delta_t \leq \delta_{tc}) \tag{4}$$

$$\tilde{T}_t = 0 \quad (\Delta_t > \delta_{tc}) \tag{5}$$

where  $z = 16e/9$ ,  $e = \exp(1)$ ,  $\tilde{\tau}_{\max}$  is the cohesive strength under shear loading and  $\delta_{tc}$  is the critical tangential displacement jump. The hat over the cohesive-zone quantities represents interfacial parameters where viscoelasticity is not considered.

In this model, the macroscopic mechanical property of an adhesive layer can be modeled by a constitutive law where the level of stress depends on the deformation of the adhesive layer and a time-dependent constant coefficient is included. Under monotonically increasing loading, the stress first increases, to the maximum,  $\tilde{\tau}_{\max}$ , at which damage takes place, the stress then decreases. When the deformation has increased to a critical value,  $\delta_{tc}$ , the stress reaches zero. At this point, crack growth takes place and failure of adhesive structure is formed. For adhesive structure, it is convenient to enable the constitutive relation representing the mechanical behavior of the entire adhesive layer. Such a constitutive relation describes activities in the adhesive layer before and at fracture.

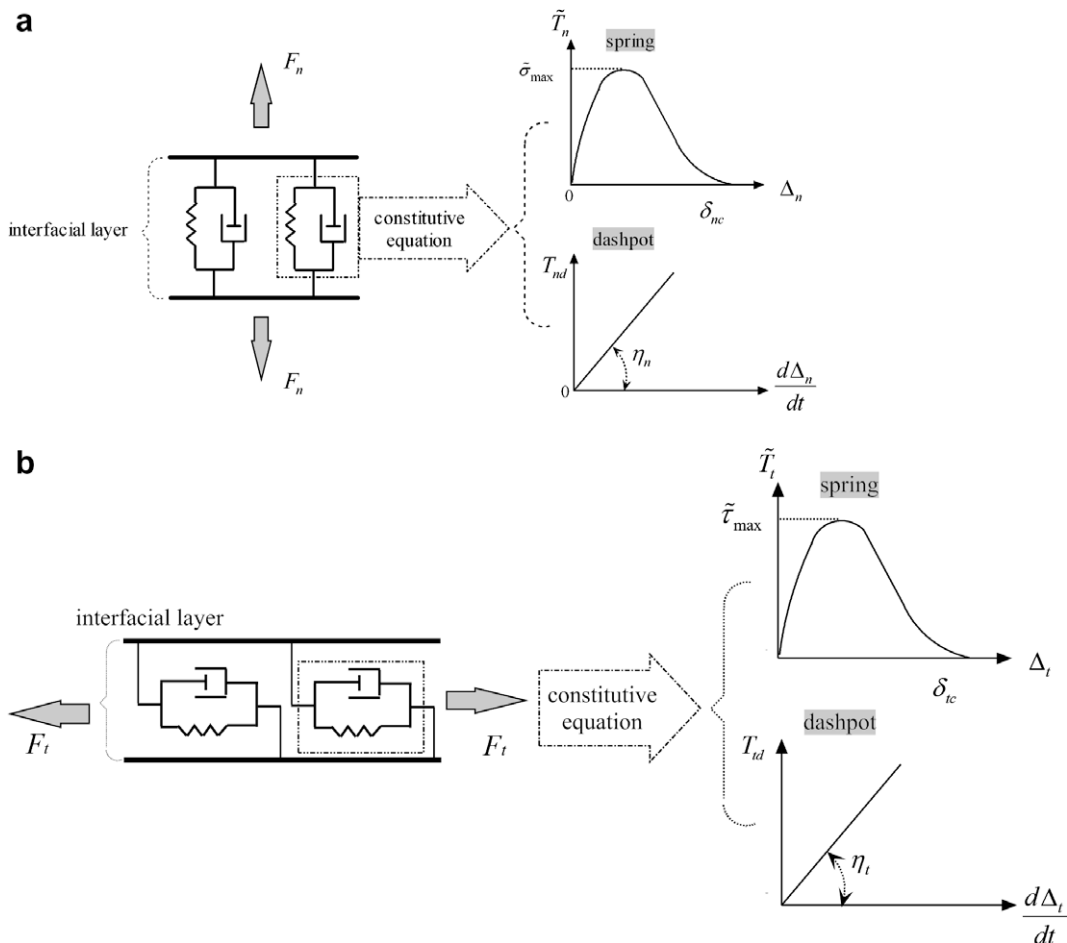


Fig. 1. The viscoelastic adhesive interfacial layer model.

Similar, the constitutive relation of viscoelastic adhesive interfacial layer model in normal direction can be expressed as

$$T_n = \tilde{T}_n + \eta_n \frac{dA_n}{dt} \quad (6)$$

where

$$\tilde{T}_n = -\tilde{\sigma}_{\max} z e^{A_n/\delta_{nc}} \exp(-zA_n/\delta_{nc}) \quad (A_n \leq \delta_{nc}) \quad (7)$$

$$\tilde{T}_n = 0 \quad (A_n > \delta_{nc}) \quad (8)$$

Then,  $\tilde{\sigma}_{\max}$  is the cohesive strength under tension loading and  $\delta_{nc}$  is the critical normal displacement jump.

The mechanical properties of the viscoelastic adhesive interfacial layer model in tangential or normal direction can be characterized by three parameters, respectively, namely interfacial strength limit,  $\tilde{\tau}_{\max}/\tilde{\sigma}_{\max}$ , displacement jump,  $\delta_{tc}/\delta_{nc}$ , and viscosity coefficient,  $\eta_t/\eta_n$ . In this model, the action of dashpot is time-dependent and its viscosity coefficient is assumed to be constant; the action of Needleman's model is time-independent and its strength limit and displacement jump are also constants. Thus, based on the Needleman's cohesive model, a three-parameter interfacial constitutive model is constructed to investigate deformation, damage and debonding behavior of the adhesive layer in adhesive structure. In addition, it is convenient to characterize the mechanical behavior of the adhesive layer from the experimental measurement during engineering application through the parameterized interfacial model. In the following analysis the vectors containing the three unknown interfacial parameters, such as,  $\mathbf{r}(\tilde{\tau}_{\max}, \delta_{tc}, \eta_t)$  for shear loading and  $\mathbf{s}(\tilde{\sigma}_{\max}, \delta_{nc}, \eta_n)$  for tension loading in adhesive layer of metal adhesive structure and rubber adhesive structure, are identified with the following improved experiment-based identification method, respectively.

### 3. Improved experiment-based identification method

In this section the improved experiment-based identification method is developed for the determination of viscoelastic adhesive interfacial mechanical properties of adhesive structures under tension and shear loading. The interfacial mechanical properties identification problem to be considered is based on the experimental measurement, to seek such an interfacial parameter vector in the solution space that the deformation and failure information in adhesive layer obtained from the numerical simulation is in a good agreement with or convergent to the related experimental results.

In this method, there are four main components: (1) numerical calculations based on the proposed viscoelastic interfacial layer model; (2) experimental measurement under tension or shear loading in real time; (3) an appropriate optimization technique, and (4) the independent experimental verification. To identify the unknown parameter vector  $\mathbf{r}(\tilde{\tau}_{\max}, \delta_{tc}, \eta_t)$  and  $\mathbf{s}(\tilde{\sigma}_{\max}, \delta_{nc}, \eta_n)$ , the whole procedure of the proposed method is performed iteratively: firstly, the initial interfacial properties, which are expressed in terms of a set of unknown parameters, are calculated employing a finite element computer program.

The viscoelastic adhesive interfacial behavior can be represented by the constitutive relation of the proposed adhesive interfacial model. While the deformation, damage and failure of the adhesive layer can be simulated numerically. At the same time, the corresponding experimental response of the shear and tension specimens is recorded. To identify the viscosity parameter ( $\eta_n$  or  $\eta_t$ ), a video-recorded data acquisition system is designed to obtain the real-time deformation and damage information of the adhesive layer. Using the results from experimental measurement and simulation calculation, an objective function is constructed and minimization of the objective function with respect to the unknown vector  $\mathbf{r}$  or  $\mathbf{s}$  is performed by means of an improved genetic algorithm. The optimal interfacial layer parameter vector  $\mathbf{r}^*(\tilde{\tau}_{\max}, \delta_{tc}, \eta_t)$  or  $\mathbf{s}^*(\tilde{\sigma}_{\max}, \delta_{nc}, \eta_n)$  can thus be obtained through the inverse process. Finally, an independent experiment is proposed and conducted to verify the identified results. The logical flowchart of the experiment-based hybrid/inverse analysis is shown in Fig. 2.

### 4. Identification of viscoelastic adhesive interfacial mechanical properties

In this section, the viscoelastic adhesive interfacial mechanical properties of metal adhesive structure (elastic material) and rubber adhesive structure (hyperelastic material) under tension and shear loading, respectively, are quantitatively characterized using the proposed experiment-based identification method. In the analysis, identification process of the rubber adhesive structure specimen under tension loading is performed in detail. Furthermore, the rubber specimen under shear loading and the metal adhesive structure specimen under shear and tension loading are also considered.

#### 4.1. Experimental test

The rubber adhesive specimens used in the tension loading are shown schematically in Fig. 3. The specimens were loaded through an Instron 3343 mechanical testing machine at constant loading speeds of 0.3, 0.5 and 1.0 mm/s under tension loading. In addition, to facilitate in-situ optical observations during the deformation process, a marker technique was adopted and uniform square grids were printed on the free surface of the specimen with the density of 2 lines/mm. A high-resolution CCD (Basler A202k with the resolution up to 1004 × 1004 and the length of a pixel is 7.4 μm) coupled with a video-recorded image data acquisition system (Matrox meteor II Camera link) was used to measure the actual displacement of the specimen. Thus, the local deformation and the processes of failure initiation and propagation in the adhesive layer were recorded in real time.

Employing the video-recorded image acquisition system, the deformation and damage information of the adhesive interface were recorded for a rubber adhesive structure specimen under tension loading (at constant loading speed of  $v = 1.0$  mm/s), the deformation images of  $t = 4$  s and 12 s are shown in Fig. 4. It can be seen from

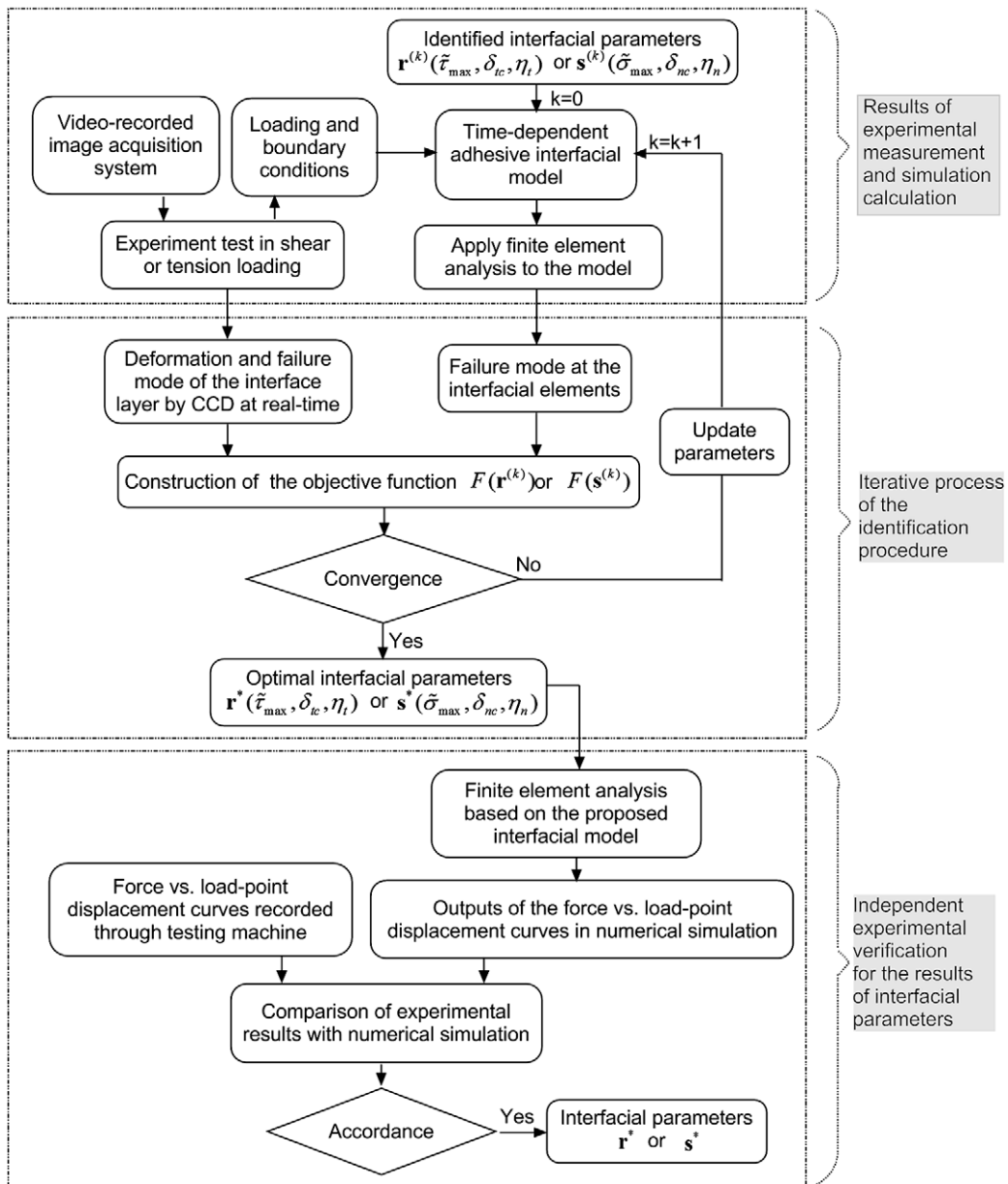


Fig. 2. Flowchart of the improved experiment-based identification method.

these images that the failure of the specimen during the deformation process is a kind of peel failure at the interface of the adhesive structure. By means of these deformation images, the position of the failure at the adhesive interface can be recorded in real time, which is important for constructing the objective function of the identification problem.

With the same apparatus, the shear experiment of rubber adherend was loaded at constant loading speeds of 1.0, 1.5 and 2.0 mm/s. For metal specimen, two LY12-CZ aluminum alloy adherends (Young's modulus  $E = 71$  GPa, Poisson's ratio  $\nu = 0.33$ ) were coated with adhesive (WL-506) at room temperature. The specimen was loaded through

an Instron 3343 mechanical testing machine at constant loading speeds of 0.02, 0.1 and 0.2 mm/s under shear loading and at constant loading speeds of 0.02, 0.2, 1.0 and 2.0 mm/s under tension loading, respectively.

#### 4.2. Numerical simulation

Numerical simulation plays an important role in the experiment-based identification method. Numerical prediction of the interfacial behavior and the corresponding experimental results are two important components of the proposed identification method. The interfacial damage is numerically simulated by means of ABAQUS (2001)

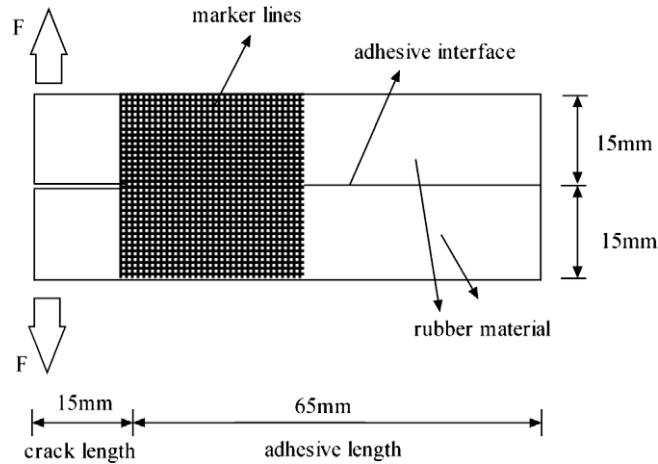


Fig. 3. Tension specimen of rubber adhesive structure.

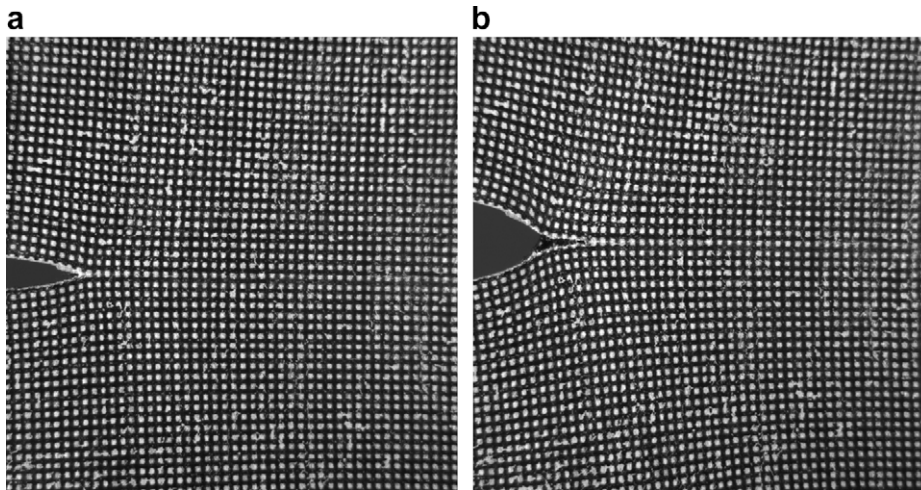


Fig. 4. Deformation images of rubber specimen under tension loading at  $v = 1.0$  mm/s.

and its user-defined subroutine capability. The time-dependent interfacial elements have four nodes and the corresponding integration is carried out at two integration points. The continuum elements for the adherends are four-node bilinear elements. Adjacent to the interfacial elements, representing the adhesive interfacial layer, one row of square solid elements is located. Subsequently, the size of the elements is gradually increased with increased distance from the interfacial elements. The initial size of the square elements and the size of the interfacial elements is 0.1 mm. In the numerical calculations, the proposed viscoelastic adhesive interfacial constitutive model was implemented into the finite element software ABAQUS/Standard (2001) by means of a user-defined element subroutine, to define the interaction behavior of the adhesive interfacial layer. It should be mentioned that the proposed element is a two-dimensional element with four nodes and zero initial thickness. Before deformation the element nodes of the upper face coincide with the corresponding nodes of the lower face. In this paper, only one displacement degree of freedom at each node is consid-

ered. It is the one along the normal direction under tension loading or along the tangential direction under shear loading. As the continuum elements connected to the interface element may deform, the displacement between the upper and lower faces increases from zero and follows the assumed traction-displacement relationship in Eq. (3) under shear loading or Eq. (6) under tension loading. The bulk elements for the adherend are four-node bilinear elements. The material properties used in the analysis for aluminum alloy are  $E = 71$  GPa and  $\nu = 0.33$ . For rubber material several non-linear constitutive laws represented by hyperelasticity have been incorporated in ABAQUS. A Van der Waals material model is used here and is defined by

$$U = \mu \left\{ -(\lambda_m^2 - 3)(\log(1 - \eta) + \eta) - \frac{2}{3} \alpha \left( \frac{I_1 - 3}{2} \right)^{\frac{3}{2}} \right\} \quad (9)$$

where  $\eta = \left( \frac{I_1 - 3}{\lambda_m - 3} \right)^{\frac{1}{2}}$ .  $\lambda_m$ ,  $\mu$ , and  $\alpha$  are material parameters which can be determined through experimental tests. For the specimen used in this work, the material parameters

of rubber are  $\lambda_m = 663.29$ ,  $\mu = 0.877$ , and  $\alpha = 4.72 \times 10^{-2}$ . Four different mesh densities are used to study the convergence of the numerical simulation.

### 4.3. Objective function

For a given identification problem, it is important to construct a reasonable objective function which is sensitive to the parameters to be identified. To reduce the effects of the noise during the tests, the failure region and the damage state of the interfaces are introduced to the objective function as base variables. In the experiment, the grid technique was used to mark damage state of the interfacial layer by the gap between the two surfaces. Construction of the objective function is as follows. First, a number  $i$  ( $i = 1, 2, \dots, p$ ) is allocated to each of the adhesive layer elements. Let  $m_i(\mathbf{e}, t)$  and  $\bar{m}_i(t)$  ( $i = 1, 2, \dots, p$ ) stand for the damage variable state of the  $i$ th adhesive layer element in the simulation calculation and the experimental results at the same moment  $t$ , respectively. It is assumed that  $m_i(\mathbf{e}, t)$  or  $\bar{m}_i(t)$  equals 0, when the damage occurs in the  $i$ th element, otherwise  $m_i(\mathbf{e}, t)$  or  $\bar{m}_i(t)$  equals 1. At the same time, a new function  $\Theta(m_i(\mathbf{e}, t), \bar{m}_i(t))$  is presented, representing the difference in the damage variable state obtained from numerical calculation and experimental observation, with the assumption that  $\Theta(m_i(\mathbf{e}, t), \bar{m}_i(t))$  equals 0 in the case of  $m_i(\mathbf{e}, t) = \bar{m}_i(t)$ , otherwise it equals 1. From the above discussion, considering a given period of time, say  $q$ , the objective function and the optimization problem can, respectively, be shown as

$$F(\mathbf{e}) = \sum_{t=1}^q \sum_{i=1}^p \Theta[m_i(\mathbf{e}, t), \bar{m}_i(t)] \quad (10)$$

Under shear loading,  $\mathbf{e} = \mathbf{r}(\bar{\tau}_{\max}, \delta_{tc}, \eta_t)$ , the objective function can be expressed as

$$F(\mathbf{r}) = \sum_{t=1}^q \sum_{i=1}^p \Theta[m_i(\mathbf{r}, t), \bar{m}_i(t)] \quad (11)$$

$$\mathbf{r}^* = \arg \min_{\mathbf{r} \in \mathbf{R}} F(\mathbf{r}) \quad (12)$$

where  $\mathbf{r}^*$  represents the optimal interfacial layer parameters vector of adhesive interfacial layer in three-dimensional space  $R(\bar{\tau}_{\max}, \delta_{tc}, \eta_t)$  under shear loading.

Similarly, under tension loading noting that  $\mathbf{e} = \mathbf{s}(\bar{\sigma}_{\max}, \delta_{nc}, \eta_n)$ , the corresponding objective function can be written as

$$F(\mathbf{s}) = \sum_{t=1}^q \sum_{i=1}^p \Theta[m_i(\mathbf{s}, t), \bar{m}_i(t)] \quad (13)$$

$$\mathbf{s}^* = \arg \min_{\mathbf{s} \in \mathbf{S}} F(\mathbf{s}) \quad (14)$$

where  $\mathbf{s}^*$  represents the optimal interfacial layer parameters vector of adhesive interfacial layer in three-dimensional space  $S(\bar{\sigma}_{\max}, \delta_{nc}, \eta_n)$  under tension loading.

### 4.4. Identification of viscoelastic interfacial layer parameters by genetic algorithm

It is noted that some challenging problems exist in solving an inverse problem as inverse problems are usually

highly non-linear and ill-posed (Liu and Han, 2003). Therefore, in many cases, traditional inverse techniques such as the gradient-based optimization method are not suitable for solving a complex inverse problem. It can be seen from Eq. (10) that the objective function employed is a discrete function for evaluating the fitness of individuals. For discrete function, it is very difficult to calculate its derivative. Such derivative is, however, necessary to the gradient-based search method (Liu and Han, 2003). To by pass this problem, an advanced inverse technique based on a genetic algorithm is used in the inverse analysis. The genetic algorithm was introduced by Holland (1975) as a method for searching the global optimum of a complicated problem. The concept of genetic algorithm originates from the principles of Charles Darwin's theory of biological evolution (Goldberg, 1989; Michalewicz, 1994). According to the algorithm, individuals are produced through three stochastic operations: selection, crossover, and mutation. The primitive genes of individuals are selected randomly according to the genetic operators. The crossover operator recombines a pair of individuals into two new individuals, and the mutation operator alters a single individual by changing its genes with the given probability, respectively. Individuals are evaluated using fitness function which is called objective function in the inverse problem. The candidates with better fitness are selected for reproduction which replaces the solutions with worse fitness. The previous studies showed that genetic algorithm is promising in dealing with large, discrete, non-linear and poorly understood optimization problem, where expert knowledge is scarce or difficult to obtain. The method has been widely accepted as optimization methods in various fields, such as flaw detection (Liu and Chen, 2001; Perera and Torres, 2006), interfacial parameter identification (Lin et al., 2005), material properties determination (Cunha et al., 1999; Chakraborty et al., 2002; Vishnuvardhan et al., 2008) and parameter calibration (Koh et al., 2003; Salomonsson and Andersson, 2008).

In this study, the optimization procedure for identifying parameters of viscoelastic adhesive interfacial structures was programmed in MATLAB 7, which required the preparation of a vast amount of input data from ABAQUS solver. Finally, at given loading speed, through a series of experiments and algorithm performance comparisons, the population size of each generation is set as 30 and the probabilities of crossover and mutation were set to 0.8 and 0.05, respectively. The optimum value could be obtained after 100 generations (the genetic parameter which represents the maximum number of operations).

The history of fitness value under tension loading in rubber material, normalized to the range of 0–1 by the number of interfacial elements of the model, against the number of generations for a genetic algorithm run is plotted in Fig. 5. It is observed from the convergence curve that the genetic algorithm converges very quickly at the beginning and slows significantly at the final stage of searching.

Finally, the identifying values of the three interfacial layer parameters of different materials (rubber or aluminum alloy) under tension loading and shear loading are shown in Table 1. In comparison with the interfacial layer

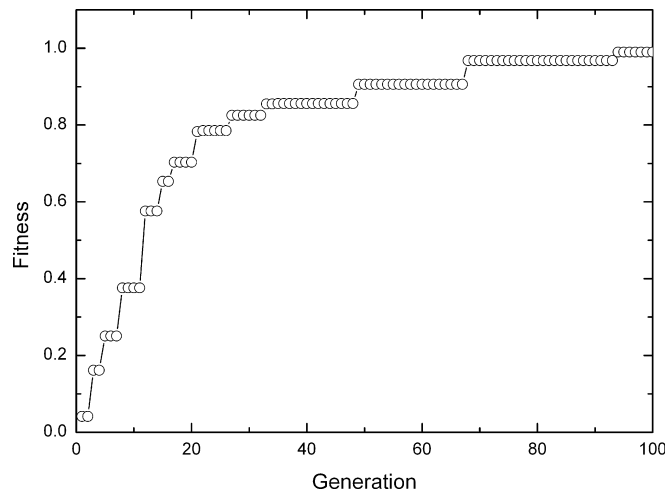


Fig. 5. History of the fitness value under tension loading in rubber material.

Table 1

Identification results of viscoelastic adhesive interfacial model.

Parameters	Tension			Shear		
	$\bar{\sigma}_{\max}$ (MPa)	$\delta_{nc}$ (mm)	$\eta_n$ (MPa s/mm)	$\bar{\tau}_{\max}$ (MPa)	$\delta_{tc}$ (mm)	$\eta_t$ (MPa s/mm)
Rubber	7.4	0.68	19.5	16.3	1.19	20.1
Aluminum alloy	8.1	0.35	15.2	19.4	1.02	15.7

parameters of different materials (Table 1), it can be seen that:

- The strength and stiffness of the interface are mode-dependent. For the interfacial mechanical property of the rubber adhesive structure, the interfacial shear strength,  $\bar{\tau}_{\max}$ , is much higher than the interfacial tensile strength,  $\bar{\sigma}_{\max}$  ( $\bar{\tau}_{\max} \approx 2.3\bar{\sigma}_{\max}$  here). The shear stiffness of the interface  $\delta_{tc}$  is higher than its tensile stiffness  $\delta_{nc}$  ( $\delta_{tc} \approx 2\delta_{nc}$  in this work). Moreover, for the interfacial mechanical properties of the aluminum alloy adhesive structure, the similar trend can be observed from Table 1. It is noted that the fracture energy of the adhesive structure loaded in shear is higher than that loaded in tension. Thus, in engineering application, the structures are often designed to be loaded in shear.
- The time-dependent viscosity coefficient of adhesive structure is mode-independent. For the rubber adhesive structure, there is little difference between the viscosity coefficient  $\eta_t$  (loaded in shear) and  $\eta_n$  (loaded in tension) within the adhesive interfacial layer. The similar conclusion can be obtained from the results for aluminum alloy adhesive structure. Thus, for a given adhesive structure (either elastic material or hyperelastic material), the time-dependent viscosity coefficient is insensitive to the loading mode. Considering the mode-independent property, the viscosity coefficient under mixed loading can be obtained from the identification results under either shear loading or tensile loading.

- The interfacial mechanical property is relative to the material property of adhesive structure. For the interfacial mechanical property of different adhesive structures under same loading condition (shear loading or tensile loading), the interfacial strength of aluminum alloy adherend (elastic) is higher than the corresponding one of rubber adherend (hyperelastic). However, the interfacial stiffness and viscosity coefficient of aluminum alloy adhesive structure are lower than those of rubber adhesive structure. This might be due to the fact that, during the loading process, the deformation of the adherend might weaken the loading on the adhesive interface. For rubber adherend, there was more deformability than aluminum alloy adherend.

## 5. Discussion and conclusions

Viscoelastic shear interfacial parameters of the adhesive layer are identified by the improved experiment-based identification method based on the loading speed ( $v = 1.0$  mm/s). However, for the experiment-based identification analysis method, problems such as unstable solution or multi-solution of the parameters may exist in the inverse process. To overcome this problem and to identify the viscoelastic interfacial parameters correctly, an independent experimental verification method is developed. In this method, the independent experimental measurement at other loading speeds and the corresponding numerical simulation with the interfacial parameters iden-

tified at loading  $v = 1.0$  mm/s are included. Firstly, two other loading speeds ( $v = 0.3$  mm/s and  $v = 0.5$  mm/s) are carried out as the verification experiments under the same experimental condition described in Section 4. Subse-

quently, compared the experimental results at  $v = 0.3$  mm/s and  $v = 0.5$  mm/s loading speeds with the numerical simulation ones based on the interfacial parameters identified above. The results are presented in Fig. 6(a).

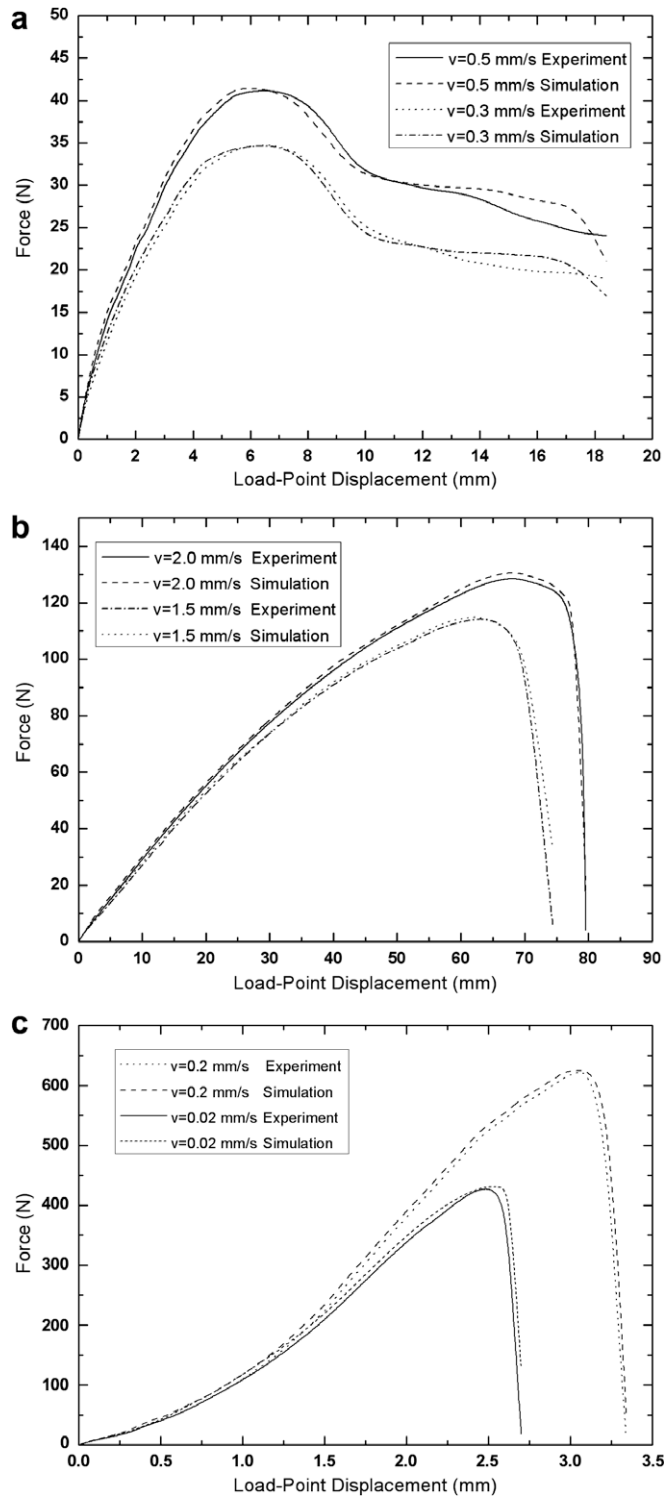


Fig. 6. Results of experiment versus numerical simulation of independent experimental verification.

It can be seen from Fig. 6(a) that the curves from experiment and simulation at the same loading speed provide satisfactory coincidence and the results of the identified parameters are effective at given loading speeds. The results for interfacial layer parameters of adhesive layer identified at the loading speed  $v = 1.0$  mm/s are in good agreement with those from the other two loading conditions. Similar results of rubber adhesive structure under shear loading can be observed from Fig. 6(b). For aluminum alloy adhesive structure, the results of independent experimental verification under shear loading is shown in Fig. 6(c).

From the discussion above, it is reasonable for the mechanical parameters identified to characterize the properties of the adhesive layer. The three-parameter viscoelastic adhesive interfacial model developed in this paper is thus effective for analyzing time-dependent adhesive structures and can be used to quantitatively characterize viscoelastic mechanical properties of the adhesive layer under shear loading and tension.

In this paper, a three-parameter interfacial model based on Needleman's cohesive theory was proposed to simulate the viscoelastic interfacial mechanical property of adhesive structure. In this model, the deformation, damage and debonding behavior of the adhesive layer can be characterized in terms of interfacial strength limit,  $\bar{\tau}_{\max}/\bar{\sigma}_{\max}$ , displacement jump,  $\delta_{tc}/\delta_{nc}$ , and viscosity coefficient,  $\eta_t/\eta_n$ . An experiment-based identification procedure including full-field real-time measurements, finite element simulation, global optimization and independent verification is presented. The procedure is then used to identify quantitatively interfacial layer mechanical parameters of the aluminum alloy adhesive structure or rubber adhesive structure under tensile and shear loading conditions, which are difficult to measure directly from experiment. In particular, the improved experiment-based identification method can be further extended for solving complex, non-linear, real-time and multi-parameter identification problems of actual adhesive structures.

## Acknowledgements

The authors would like to thank Professor K.H. Laermann (Bergische Universität-GH Wuppertal, D-42285 Wuppertal, Germany) for his useful discussion in hybrid/inverse method and would like to acknowledge the support from the National Science Foundation of China (No. 10572102) and National Basic Research Program of China (No. 2007CB714000). J. Wang is also grateful to support from the China Scholarship Council.

## References

- ABAQUS/Standard User's Manual for Version 6.2, 2001. Hibbit, Karlsson & Sorensen, Inc., Pawtucket, RI.
- Alfredsson, K.S., 2003. On the determination of constitutive properties of adhesive layers loaded in shear – an inverse solution. *Int. J. Fract.* 123 (1–2), 49–62.
- Asundi, A., 1999. Hybrid methods. *Opt. Lasers Eng.* 32, 181–182.
- Balakrishnan, A., Socrate, S., 2008. Material property differentiation in indentation testing using secondary sensors. *Exp. Mech.* 48, 549–558.
- Chakraborty, S., Mukhopadhyay, M., Sha, O.P., 2002. Determination of physical parameters of stiffened plates using genetic algorithm. *J. Comput. Civil Eng.* 16, 206–221.
- Chalal, H., Meraghni, F., Pierron, F., Grediac, M., 2004. Direct identification of the damage behaviour of composite materials using the virtual fields method. *Compos. Part A* 35 (7–8), 841–848.
- Cooreman, S., Lecompte, D., Sol, H., Vantomme, J., Debruyne, D., 2007. Elasto-plastic material parameter identification by inverse methods: calculation of the sensitivity matrix. *Int. J. Solids Struct.* 44 (13), 4329–4341.
- Cosola, E., Genovese, K., Lamberti, L., Pappalettere, C., 2008. A general framework for identification of hyper-elastic membranes with moiré techniques and multi-point simulated annealing. *Int. J. Solids Struct.* 45 (24), 6074–6099.
- Cunha, J., Cogan, S., Berthod, C., 1999. Application of genetic algorithms for the identification of elastic constants of composite materials from dynamic tests. *Int. J. Numer. Meth. Eng.* 45, 891–900.
- Davendralingam, N., Doyle, J.F., 2008. Nonlinear identification problem under large deflections. *Exp. Mech.* 48, 529–538.
- Du, J., Thouless, M.D., Yee, A.F., 2000. Effects of rate on crack growth in a rubber-modified epoxy. *Acta Mater.* 48, 3581–3592.
- Goldberg, D.E., 1989. *Genetic Algorithm in Search Optimization and Machine Learning*. Addison-Wesley, Reading, MA.
- Gustafson, P.A., Waas, A.M., 2009. The influence of adhesive constitutive parameters in cohesive zone finite element models of adhesively bonded joints. *Int. J. Solids Struct.* 46, 2201–2215.
- Hartmann, S., Gimmeier, J., Scholtes, B., 2006. Experiments and material parameter identification using finite elements. Uniaxial tests and validation using instrumented indentation tests. *Exp. Mech.* 46 (1), 5–18.
- Holland, J.H., 1975. *Adaptation in Natural and Artificial Systems*. The University of Michigan Press, Ann Arbor.
- Jagota, A., Bennison, S.J., Smith, C.A., 2000. Analysis of a compression shear test for adhesion between elastomeric polymers and rigid substrates. *Int. J. Fract.* 104 (2), 105–130.
- Jiang, C., Liu, G.R., Han, X., 2008. A novel method for uncertainty inverse problems and application to material characterization of composites. *Exp. Mech.* 48, 539–548.
- Kafkalidis, M.S., Thouless, M.D., 2002. The effects of geometry and material properties on the fracture of single lap-shear joints. *Int. J. Solids Struct.* 39, 4367–4383.
- Kang, Y.L., Lin, X.H., Qin, Q.H., 2004. Inverse/genetic method and its application in identification of mechanical parameters of interface in composite. *Compos. Struct.* 66, 449–458.
- Kobayashi, A.S., 1983. Hybrid experimental–numerical stress analysis. *Exp. Mech.* 23 (3), 338–347.
- Kobayashi, A.S., 1987. *Handbook on Experimental Mechanics*. Prentice-Hall, Inc., London.
- Koh, C.G., Chen, Y.F., Liaw, C.Y., 2003. A hybrid computational strategy for identification of structural parameters. *Comput. Struct.* 81, 107–117.
- Laermann, K.H., 1981. Hybrid analysis of plate problems. *Exp. Mech.* 21 (10), 386–388.
- Landis, C.M., Pardoan, T., Hutchinson, J.W., 2000. Crack velocity dependent toughness in rate dependent materials. *Mech. Mater.* 32, 663–678.
- Leffler, K., Alfredsson, K.S., Stigh, U., 2007. Shear behaviour of adhesive layers. *Int. J. Solids Struct.* 44 (2), 530–545.
- Li, S., Thouless, M.D., Waas, A.M., Schroeder, J.A., Zavattieri, P.D., 2005a. Use of mode-I cohesive-zone models to describe the fracture of an adhesively-bonded polymer–matrix composite. *Compos. Sci. Technol.* 65, 281–293.
- Li, S., Thouless, M.D., Waas, A.M., Schroeder, J.A., Zavattieri, P.D., 2005b. Use of a cohesive-zone model to analyze the fracture of a fiber reinforced polymer–matrix composite. *Compos. Sci. Technol.* 65, 537–549.
- Liechti, K.M., Wu, J.D., 2001. Mixed-mode, time-dependent rubber/metal debonding. *J. Mech. Phys. Solids* 49, 1039–1072.
- Lin, X.H., Kang, Y.L., Qin, Q.H., Fu, D.H., 2005. Identification of interfacial parameters in a particle reinforced metal matrix composite Al6061–10%Al<sub>2</sub>O<sub>3</sub> by hybrid method and genetic algorithm. *Comput. Mater. Sci.* 32 (1), 47–56.
- Liu, G.R., Chen, S.C., 2001. Flaw detection in sandwich plates based on time-harmonic response using genetic algorithm. *Comput. Methods Appl. Mech. Eng.* 190 (42), 5505–5514.
- Liu, G.R., Han, X., 2003. *Computational Inverse Techniques in Nondestructive Evaluation*. CRC Press, Boca Raton, FL.
- Michalewicz, Z., 1994. *Genetic Algorithm + Data Structures = Evolution Programs*. Springer-Verlag, New York.

- Molimard, J., Riche, R.L., Vautrin, A., Lee, J.R., 2005. Identification of the four orthotropic plate stiffnesses using a single open-hole tensile test. *Exp. Mech.* 45 (5), 404–411.
- Needleman, A., 1990. An analysis of decohesion along an imperfect interface. *Int. J. Fract.* 42 (1), 21–40.
- Perera, R., Torres, R., 2006. Structural damage detection via modal data with genetic algorithms. *J. Struct. Eng.* 132, 1491–1501.
- Salomonsson, K., Andersson, T., 2008. Modeling and parameter calibration of an adhesive layer at the meso level. *Mech. Mater.* 40 (1–2), 48–65.
- Thouless, M.D., Waas, A.M., Schroeder, J.A., Zavattieri, P.D., 2006. Mixed-mode cohesive-zone models for fracture of an adhesively bonded polymer–matrix composite. *Eng. Fract. Mech.* 73, 64–78.
- Tvergaard, V., Hutchinson, J.W., 1993. The influence of plasticity on the mixed-mode interface toughness. *J. Mech. Phys. Solids* 41, 1119–1135.
- Tvergaard, V., Hutchinson, J.W., 1996. On the toughness of ductile adhesive joints. *J. Mech. Phys. Solids* 44, 789–800.
- Vishnuvardhan, J., Krishnamurthy, C.V., Balasubramaniam, K., 2008. Determination of material symmetries from ultrasonic velocity measurements: a genetic algorithm based blind inversion method. *Compos. Sci. Technol.* 68 (3–4), 862–871.
- Wang, J., Kang, Y.L., Qin, Q.H., Fu, D.H., Li, X.Q., 2008. Identification of time-dependent interfacial mechanical properties of adhesive by hybrid/inverse method. *Comput. Mater. Sci.* 43, 1160–1164.
- Wei, Y.G., Hutchinson, J.W., 1998. Interface strength, work of adhesion and plasticity in the peel test. *Int. J. Fract.* 93, 315–333.
- Xu, C., Siegmund, T., Ramani, K., 2003a. Rate-dependent crack growth in adhesives: I. Modeling approach. *Int. J. Adhes. Adhes.* 23, 9–13.
- Xu, C., Siegmund, T., Ramani, K., 2003b. Rate-dependent crack growth in adhesives: II. Experiments and analysis. *Int. J. Adhes. Adhes.* 23, 15–22.
- Yang, Q.D., Thouless, M.D., Ward, S.M., 1999. Numerical simulation of adhesively-bonded beams failing with extensive plastic deformation. *J. Mech. Phys. Solids* 47 (6), 1337–1353.
- Yang, Q.D., Thouless, M.D., Ward, S.M., 2001. Elastic–plastic mode-II fracture of adhesive joints. *Int. J. Solids Struct.* 38 (18), 3251–3262.